

6. Slightly diminished NuA4 HAT activity is detected on the GST-GCN4 beads relative to SAGA. However, this difference does not appear to be due to a decreased interaction between NuA4 and Gcn4p (2, 28), but instead to a decrease in nucleosomal HAT activity when bound to GST-GCN4.
7. C. M. Drysdale *et al.*, *Mol. Cell. Biol.* **15**, 1220 (1995).
8. S. L. Berger *et al.*, *Cell* **70**, 251 (1992).
9. A. K. Sil *et al.*, *Mol. Cell. Biol.* **19**, 7828 (1999).
10. S. L. Berger, W. D. Cress, A. Cress, S. J. Triezenberg, L. Guarente, *Cell* **61**, 1199 (1990).
11. Complete experimental protocols and other information are available as supplementary material on Science Online at [www.sciencemag.org/cgi/content/full/292/5525/2333/DC1](http://www.sciencemag.org/cgi/content/full/292/5525/2333/DC1).
12. S. Allard *et al.*, *EMBO J.* **18**, 5108 (1999).
13. P. A. Grant, D. Schieltz, M. G. Pray-Grant, J. R. Yates, J. L. Workman, *Mol. Cell* **2**, 863 (1998).
14. A. Saleh *et al.*, *J. Biol. Chem.* **273**, 26559 (1998).
15. S. B. McMahon, H. A. Van Buskirk, K. A. Dugan, T. D. Copeland, M. D. Cole, *Cell* **94**, 363 (1998).
16. Several lines of evidence support the assumption that purified Flag-Tra1p is free of SAGA and NuA4 subunits (28). First, elution of Flag-Tra1p from MonoQ is chromatographically distinct from NuA4 and SAGA. Second, the purified protein does not contain any

- histone acetylase activity. Third, the purified Flag-Tra1p fraction does not contain the SAGA subunits Spt7p, TAF<sub>II</sub>90, Spt8p, and Ada2p and the NuA4 catalytic subunit Esa1p, as determined by Western blot analysis. Two smaller proteins at 85 and 35 kD are sometimes observed in this fraction. Mass spectrometry and Western analysis suggest that these are Tra1p breakdown products.
17. H. Lu, A. J. Levine, *Proc. Natl. Acad. Sci. U.S.A.* **92**, 5154 (1995).
18. M. Uesugi, O. Nyanguile, H. Lu, A. J. Levine, G. L. Verdine, *Science* **277**, 1310 (1997).
19. C. J. Thut, J. L. Chen, R. Klemm, R. Tjian, *Science* **267**, 100 (1995).
20. J. A. Goodrich, T. Hoey, C. J. Thut, A. Admon, R. Tjian, *Cell* **75**, 519 (1993).
21. W. Selleck *et al.*, *Nature Struct. Biol.*, in press.
22. W. Selleck, S. Tan, unpublished data.
23. N. A. Barlev *et al.*, *J. Biol. Chem.* **270**, 19337 (1995).
24. A. Henriksson *et al.*, *Mol. Cell. Biol.* **17**, 3065 (1997).
25. R. Candau, J. X. Zhou, C. D. Allis, S. L. Berger, *EMBO J.* **16**, 555 (1997).
26. R. Candau, S. L. Berger, *J. Biol. Chem.* **271**, 5237 (1996).
27. R. Balasubramanian, W. Selleck, M. G. Pray-Grant, P. Grant, S. Tan, in preparation.

28. C. Brown, J. Workman, unpublished data.
29. M. H. Jia *et al.*, *Physiol. Genomics* **3**, 83 (2000).
30. A. Eberharter, S. John, P. A. Grant, R. T. Utley, J. L. Workman, *Methods* **15**, 315 (1998).
31. P. D. Gregory, A. Schmid, M. Zavari, M. Munsterkotter, W. Horz, *EMBO J.* **18**, 6407 (1999).
32. L. Galarneau *et al.*, *Mol. Cell* **5**, 927 (2000).
33. M.-H. Kuo, J. Zhou, P. Jambeck, M. E. A. Churchill, C. D. Allis, *Genes Dev.* **12**, 627 (1998).
34. S. B. McMahon, M. A. Wood, M. D. Cole, *Mol. Cell. Biol.* **20**, 556 (2000).
35. S. C. Alley, F. T. Ishmael, A. D. Jones, S. J. Benkovic, *J. Am. Chem. Soc.* **122**, 6126 (2000).
36. Single-letter abbreviations for the amino acid residues are as follows: A, Ala; D, Asp; F, Phe; G, Gly; L, Leu; R, Arg; S, Ser; T, Thr; V, Val; and W, Trp.
37. We thank K. Neely, M. Swanson, A. Hinnebusch, F. Ishmael, R. Balasubramanian, and W. Selleck for helpful discussions and sharing of reagents. C.E.B. is supported by the Leukemia and Lymphoma Society. S.C.A. is supported by NIH grant GM19492. J.L.W. is an Associate Investigator of the Howard Hughes Medical Institute. This work was supported by a grant from NIGMS.

11 December 2000; accepted 15 May 2001

## Requirement of ERK Activation for Visual Cortical Plasticity

Graziella Di Cristo,<sup>1\*</sup> Nicoletta Berardi,<sup>2,3†</sup> Laura Cancedda,<sup>1</sup> Tommaso Pizzorusso,<sup>1,2</sup> Elena Putignano,<sup>1</sup> Gian Michele Ratto,<sup>2</sup> Lamberto Maffei<sup>1,2</sup>

Experience-dependent plasticity in the developing visual cortex depends on electrical activity and molecular signals involved in stabilization or removal of inputs. Extracellular signal-regulated kinase 1,2 (also called p42/44 mitogen-activated protein kinase) activation in the cortex is regulated by both factors. We show that two different inhibitors of the ERK pathway suppress the induction of two forms of long-term potentiation (LTP) in rat cortical slices and that their intracortical administration to monocularly deprived rats prevents the shift in ocular dominance towards the nondeprived eye. These results demonstrate that the ERK pathway is necessary for experience-dependent plasticity and for LTP of synaptic transmission in the developing visual cortex.

During development, experience exerts a strong control over formation of circuitry in sensory cortices, promoting the strengthening or weakening of synapses. For example, monocular deprivation (MD) during the critical period determines a loss of responsiveness to the deprived eye in visual cortical neurons. Molecules controlling experience-dependent plasticity during the critical period (1–3) should be regulated by electrical activity (4, 5) and by other factors, such as neurotrophins (6–8), important for cortical plasticity. Electrical activity and neurotrophins are among the strongest activators of ERK (9,

10), suggesting that ERK could act as an integrating molecule between these two regulatory mechanisms. ERK is also implicated in activity-dependent plasticity by studies of learning and memory (11–14). We investigated the role of ERK in experience-dependent plasticity of the visual cortex and on LTP, an in vitro model of activity-dependent synaptic plasticity [see Web material (15) for methods].

The effect of specific inhibitors (16) of the ERK pathway (U0126 and PD98059) on LTP induction was studied in visual cortical slices. A stimulating electrode was placed in layer IV, and field potentials (FPs) were evoked by a brief current pulse (100  $\mu$ s) delivered every 30 s and recorded in layer III (17). Stimulus intensity was  $55 \pm 9\%$  of that evoking the maximal response. In normal saline, theta burst stimulation (TBS) delivered to layer IV induced a potentiation of the response [FP amplitude 25 min after TBS (as percentage of

pre-TBS baseline),  $120.0 \pm 2.8\%$ ;  $n = 7$ ].

To assess the effects of ERK pathway inhibitors on LTP, slices obtained from the same animal (P26 to P33) were treated 10 min before TBS with the blocker or its vehicle [dimethyl sulfoxide (DMSO) 0.1%]. Administration of U0126 (20  $\mu$ M, a specific inhibitor of the upstream enzymes MEK that activate ERK) prevented LTP induction (Fig. 1): FP amplitude in U0126 treated slices remained at pre-TBS levels ( $99.4 \pm 4.3\%$ ). In contrast, control slices displayed normal LTP ( $119.1 \pm 3.7\%$ ). Change in FP amplitude 25 min after TBS is reported in Fig. 1C for each slice (U0126 treated or control). The time course of the response amplitude of U0126 treated slices differs from controls immediately after TBS delivery (Fig. 1A). The rapidity of the onset of U0126 effect suggests that ERK action is required for mechanisms of potentiation that, at least initially, are independent of gene transcription. The inhibitory effect of U0126 on LTP was not caused by reduced responses to the TBS or by antagonization of *N*-methyl-D-aspartate (NMDA)-mediated synaptic transmission, a key event for the induction of this form of LTP (15).

To exclude that LTP suppression by U0126 was due to a nonspecific interaction with molecules other than MEK, we tested a different MEK inhibitor, PD98059; 10-min incubation in 50  $\mu$ M PD98059 totally suppressed LTP induction (Fig. 1C). Thus, inhibition of ERK signalling prevented LTP induction in the layer IV–III pathway.

FPs recorded in layer III after stimulation of white matter (WM) can also be potentiated by TBS. However, unlike layer IV–III LTP, which can be elicited through the entire lifetime, WM LTP is present only during the critical period. This observation suggested that this form of synaptic plasticity might be

<sup>1</sup>Scuola Normale Superiore, Piazza Cavalieri, 7 56126 Pisa, Italy. <sup>2</sup>Istituto Neurofisiologia CNR, via Moruzzi 1, 56100 Pisa, Italy. <sup>3</sup>Dipartimento di Psicologia, Università di Firenze, 50123 Firenze, Italy.

\*Present address: Department of Neurobiology, Cold Spring Harbor Laboratory, Post Office Box 100, 1 Bungtown Road, Cold Spring Harbor, NY 11724, USA. †To whom correspondence should be addressed. E-mail: berardi@in.pi.cnr.it

## REPORTS

implicated in the activity-dependent refinement of cortical circuitry occurring during the critical period (18). TBS of WM strongly activates ERK phosphorylation in cortical cells. This effect of TBS can be blocked by U0126 and depends on NMDA receptor activation (Fig. 2A). We tested whether ERK activation is required for the induction of WM LTP. Slices obtained from P18 to P24 rats were used in pairs to study the effect of ERK inhibitors and their vehicle. Both U0126 and PD98059 blocked LTP induction after WM stimulation (Fig. 2, B through D). Average FP amplitudes in control slices were increased  $119.7 \pm 4.1\%$  of baseline amplitude 25 min after TBS. This potentiation was not present in slices treated with U0126 ( $98.1 \pm 2.3\%$ ) or PD98059 ( $99.5 \pm 3.3\%$ ). Exposure to U0126 but not PD98059 caused a small but significant ( $6.7 \pm 2.3\%$ ) depression of FP amplitude (Fig. 2B). These data indicate that the activation of ERK is also required for WM LTP, a form of plasticity that correlates with the critical period for MD and prompted us to investigate whether the ERK pathway is also involved in the mechanisms of experience-dependent plasticity in vivo.

We initially assessed whether visual experience can activate ERK; exposure to light in dark-reared rats caused a robust increase of ERK phosphorylation in the visual cortex (15). Next, we studied whether activation of the ERK cascade is necessary for experience-dependent plasticity in the visual cortex using the classical paradigm of MD during the critical period. In particular, we asked whether block of ERK by means of U0126 prevents the plastic changes induced by MD. U0126 ( $250 \mu\text{M}$ ) was continuously infused throughout the deprivation period (1 week) in the visual cortex contralateral to the deprived eye by means of osmotic minipumps. To control for the inhibitory action of U0126 in vivo, we strongly increased spontaneous activity in the visual cortex with picrotoxin (1 mM), a blocker of GABA<sub>A</sub> ( $\gamma$ -aminobutyric acid) receptor. U0126 was still effective in inhibiting ERK activation by picrotoxin 6 days after minipump implant (15).

Block of ERK activation by U0126 prevented MD effects (Fig. 3). In normal P28 rats, the overwhelming majority of visual cortical cells are binocular with a clear dominance of the contralateral eye [normal (NOR) contralateral bias index (CBI) (19),  $0.55 \pm 0.03$ ]. One week of MD at the peak of the critical period induces a strong shift of the ocular dominance distribution towards the open eye (MD, CBI =  $0.12 \pm 0.02$ ), which is significantly counteracted by U0126 (CBI =  $0.57 \pm 0.05$ ).

To test whether the effects of U0126 were specifically due to its inhibition of ERK activation, we studied whether preventing ERK

activation with a different MEK inhibitor, PD98059 ( $250 \mu\text{M}$ ), would also counteract MD effects. We found that PD98059 was

able to prevent MD effects (Fig. 3) (CBI =  $0.5 \pm 0.1$ ). In contrast to U0126 and PD98059, infusion of vehicle or of

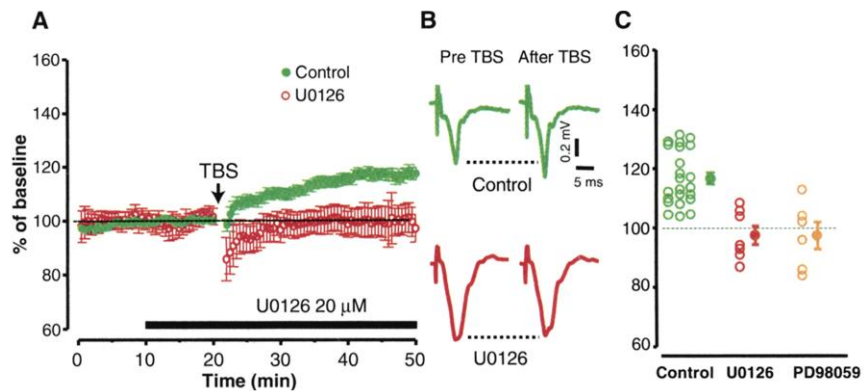


**Fig. 1.** MEK inhibitors U0126 and PD98059 prevent induction of layer IV–III LTP. (A) Average time course of layer II–III FP amplitude before and after TBS in presence of U0126 ( $n = 7$  slices) or control ( $n = 23$  slices). Time courses of slices treated with saline or the drug vehicle DMSO ( $0.1\%$ ) have been pooled together because there is no significant difference [two-way analysis of variance (ANOVA), effect of treatment and interaction time versus treatment  $P > 0.05$ ]. (B) Average of 10 traces recorded from a control and a U0126 treated slice before and 25 min after TBS. Only the control slice shows LTP. Stimulus artefacts have been partially deleted. (C) Average and single cases of LTP in control, U0126, and PD98059 slices 25 min after TBS. U0126 and PD98059 significantly prevented LTP induction (one-way ANOVA,  $P < 0.001$ ; post-hoc Tukey test DMSO versus saline  $P > 0.05$ , U0126 and PD98059 versus control  $P < 0.05$ ; PD98059 versus U0126  $P > 0.05$ ).

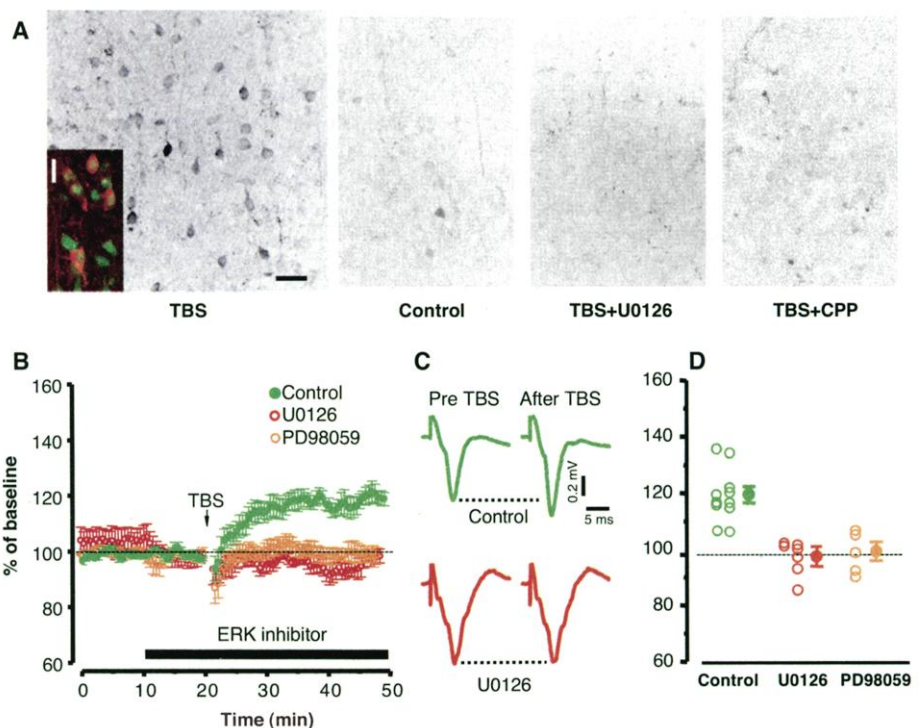


**Fig. 2.** (A) TBS causes ERK phosphorylation. Staining of phosphoERK in slices stimulated with TBS ( $n = 7$  slices), control test stimulation ( $n = 7$ ), and TBS in presence of U0126 ( $n = 5$ ) or 3-(2-carboxypiperazin-4-yl)-propyl-1-phosphonic-acid (CPP) ( $n = 2$ ), respectively. Bar,  $40 \mu\text{m}$ . Inset shows that phosphoERK staining positive cells (red) are also positive for the neuronal marker Neu-N (green). Bar,  $20 \mu\text{m}$ . (B) MEK inhibitors U0126 and PD98059 block LTP in the WM–layer III pathway. Average time course of layer III FP amplitude before and after TBS in presence of U0126 ( $n = 7$ ), PD98059 ( $n = 5$ ), or vehicle ( $n = 11$ ). U0126 and PD98059 blocked LTP induction. (C) Average of 10 traces recorded from a vehicle and a U0126 treated slice before and 25 min after TBS. (D) Average and single cases of LTP in control, U0126, and PD98059 slices 25 min after TBS. None of the slices treated with U0126 or PD98059 displayed LTP. The effect of U0126 and PD98059 was highly significant (one-way ANOVA,  $P < 0.001$ ; post-hoc Tukey test: U0126 and PD98059 versus control  $P < 0.05$ ; PD98059 versus U0126  $P > 0.05$ ).

SB203580 (250  $\mu$ M), a selective inhibitor of p38 MAPK, did not have any effect (Fig. 3) (vehicle CBI =  $0.17 \pm 0.04$ ; SB203580 CBI =  $0.18 \pm 0.03$ ). Thus, the effects of U0126 and PD98059 on ocular dominance plasticity cannot be attributed to aspecific effects of the infusion or to aspecific inhibition of kinases of the MAPK family.

The ocular dominance data for all animals recorded are summarized in Fig. 3B, and the CBI is reported for each animal. It is clear that the CBI of MD animals treated with vehicle or SB203580 is indistinguishable from that of MD untreated animals. CBI of

MD animals treated with U0126 or PD98059 do not differ from that of normal animals.

ERK is an important hub of intracellular pathways linked to activity (10), so it was important to control that blocking activation of ERK did not affect visual cortical cell electrical activity, both spontaneous and visually evoked. Indeed, any treatment that strongly alters electrical activity is bound to affect the outcome of MD. Therefore, we evaluated several functional properties of visual cortical neurons in our normal, MD, and MD treated animals. None of the treatments significantly affected spontaneous discharge, cell responsiveness, receptive field size (Fig. 4, A and B), or orientation selectivity.

To further control for possible alterations of the functional properties of visual cortical cells during treatment, we evaluated spontaneous and visually evoked activity in nondeprived animals treated with U0126 at 2 and 6 days after minipump implant. Again, U0126 treatment did not significantly alter cell responsiveness and receptive field size (Fig. 4,

C and D), which were indistinguishable from those of normal or vehicle-treated animals. Also, the ocular dominance distribution was not grossly affected, suggesting that U0126 application does not alter ocular dominance distribution. To confirm that blockage of ERK did not affect visual cortex functional development, we also determined visual acuity using VEP, a sensitive measure for the state of visual cortical development, predictive of visual behavior (20, 21). Visual acuity values of U0126 treated rats are superimposable on those of normal animals of the same age (15).

Thus, the activation of the ERK pathway seems to be specifically involved in mediating the plastic changes induced by MD, but not in regulating responsiveness to visual stimulation or in determining other response properties of visual cortical cells.

If the mechanisms at work in the *in vitro* models of plasticity we have used reflect those involved in experience-dependent plasticity, these results suggest that ERK could

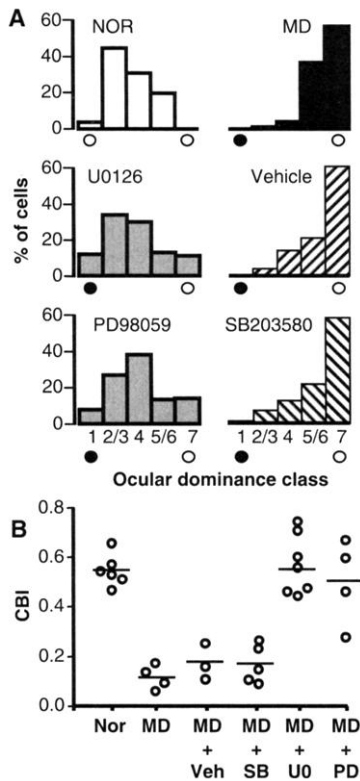


**Fig. 3.** (A) U0126 and PD98059 block the ocular dominance shift induced by MD. Ocular dominance distributions for normal P28 animals (NOR, 6 rats, 164 cells) and for animals MD from P21 to P28, either untreated (MD, 4 rats, 88 cells) or treated with: U0126 (7 rats, 168 cells), vehicle (3 rats, 73 cells), PD98059 (4 rats, 128 cells), or SB203580 (5 rats, 153 cells). Distributions for animals treated with U0126 and PD98059 significantly differ from those for untreated, vehicle and SB203580 treated animals ( $\chi^2$  test,  $\nu = 4$ ,  $P < 0.001$ ); these latter three do not differ one from each other. (B) CBI for all animals recorded in each experimental group. For each treatment group, average CBI is indicated by a horizontal line. CBI for deprived U0126 treated animals are significantly different from those obtained in untreated, vehicle, and SB203580 treated animals ( $P < 0.05$ ), whereas they are not different ( $P > 0.05$ ) from those found in normal animals or PD98059 treated MD animals. CBI for deprived animals untreated, vehicle, or SB203580 treated group together ( $P > 0.05$ ) (one-way ANOVA,  $P < 0.01$ , post-hoc Tukey test).

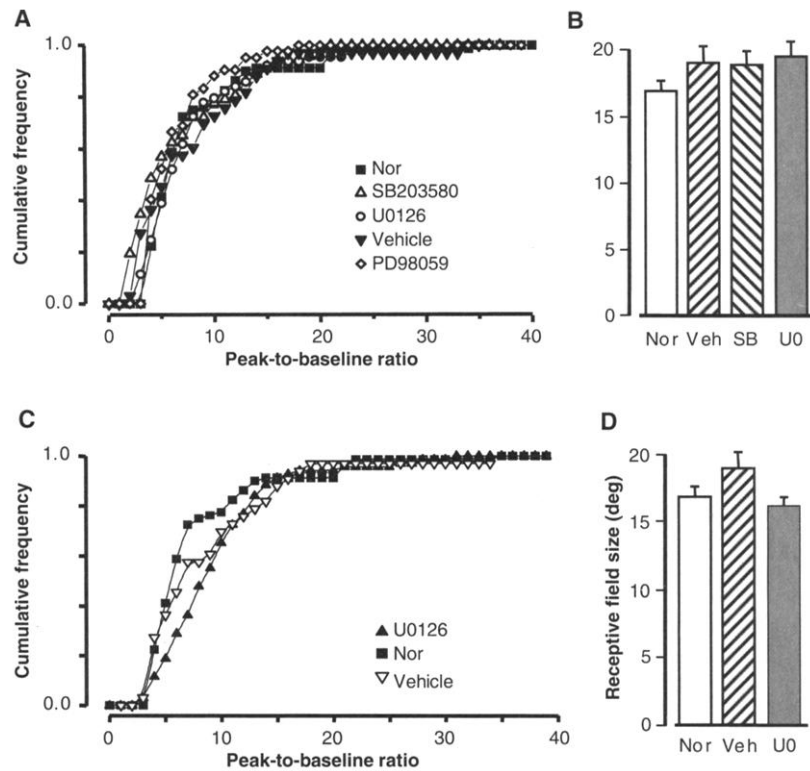


**Fig. 4.** Cell responsiveness (A) and receptive field (RF) size (B) of visual cortical neurons are normal in MD animals after 1 week of treatment with ERK inhibitors. (A) The cumulative fraction of the total number of recorded neurons is plotted against the peak-to-baseline ratio values. Normal, 81 cells; U0126, 114 cells; PD98059, 49 cells; SB203580, 72 cells; vehicle, 35 cells. No significant effect of treatment with respect to normal values [Kolmogorov-Smirnov (K-S) test]. (B) RF size for normal animals (89 cells) and MD animals treated with U0126 (45 cells), vehicle (20 cells), SB203580 (49 cells). No significant effect of treatments (one-way ANOVA,  $P > 0.05$ ). Cell responsiveness (C) and RF size (D) during U0126 treatment (2 and 6 days after minipump implant) are normal. (C) The cumulative fraction of the total number of recorded neurons is plotted against the peak-to-baseline ratio values. Normal, 81 cells; vehicle, 35 cells; U0126, 69 cells. There is no statistical difference between any of the three curves shown (K-S test). Data for U0126 collected at 2 and 6 days after implant have been pooled together, because there was no statistical difference (K-S test). (D) RF size for normal animals (81 cells), animals treated with vehicle (20 cells), or U0126 (51 cells) recorded during treatment. No significant effect of treatment (one-way ANOVA,  $P > 0.05$ ).

intervene in MD plasticity by mediating the strengthening of active inputs. The existing information allows envisioning two mechanisms by which ERK could exert its actions on activity-dependent synapse strengthening. First, phosphorylated ERK could, at synaptic level, modulate the activity of substrates important for plasticity such as synaptic proteins (22), ionic channels (23), or adhesion molecules (24). A second mode of action involves translocation of phosphorylated ERK to the nucleus where it activates, directly or through kinases of the p90 ribosomal S6 kinase family, various transcription factors crucial for plasticity (25, 26).

# References and Notes

1. N. Berardi, T. Pizzorusso, L. Maffei, *Curr. Opin. Neurobiol.* **10**, 138 (2000).
2. T. K. Hensch et al., *Science* **282**, 1504 (1998).
3. M. Fagioli, T. K. Hensch, *Nature* **404**, 183 (2000).
4. E. M. Quinlan, B. D. Philpot, R. L. Huganir, M. F. Bear, *Nature Neurosci.* **2**, 352 (1999).
5. S. Glazewski, K. P. Giese, A. Silva, K. Fox, *Nature Neurosci.* **3**, 911 (2000).
6. C. Lodovichi, N. Berardi, T. Pizzorusso, L. Maffei, *J. Neurosci.* **20**, 2155 (2000).
7. A. K. McAllister, L. C. Katz, D. C. Lo, *Annu. Rev. Neurosci.* **22**, 295 (1999).
8. Z. J. Huang et al., *Cell* **98**, 739 (1999).
9. T. Pizzorusso, G. M. Ratto, E. Putignano, L. Maffei, *J. Neurosci.* **20**, 2809 (2000).
10. S. S. Grewal, R. D. York, P. J. Stork, *Curr. Opin. Neurobiol.* **9**, 544 (1999).
11. G. E. Schafe et al., *J. Neurosci.* **20**, 8177 (2000).
12. S. Blum, A. N. Moore, F. Adams, P. K. Dash, *J. Neurosci.* **19**, 3535 (1999).
13. D. E. Berman, S. Hazvi, K. Rosenblum, R. Seger, Y. Dudai, *J. Neurosci.* **18**, 10037 (1998).
14. C. M. Atkins, J. C. Selcher, J. J. Petraitis, J. M. Trzaskos, J. D. Sweatt, *Nature Neurosci.* **1**, 602 (1998).
15. Web figures 1 through 4 and text on methods are available at *Science* Online at [www.sciencemag.org/cgi/content/full/292/5525/2337/DC1](http://www.sciencemag.org/cgi/content/full/292/5525/2337/DC1).
16. S. P. Davies, H. Reddy, M. Caivano, P. Cohen, *J. Biochem.* **351**, 95 (2000).
17. A. Kirkwood, M. F. Bear, *J. Neurosci.* **14**, 1634 (1994).
18. A. Kirkwood, H. K. Lee, M. F. Bear, *Nature* **375**, 328 (1995).
19. For each animal the bias of the ocular dominance distribution towards the contralateral eye was calculated using a CBI.  $CBI = \frac{[N(1) - N(7)] + 1/2[N(2/3) - N(5/6)] + N(tot)/2N(tot)}{N(tot)}$ , where  $N(tot)$  is the total number of recorded cells and  $N(i)$  is the number of cells in class (i).
20. D. Birch, G. H. Jacobs, *Vision Res.* **19**, 933 (1979).
21. M. Fagioli, T. Pizzorusso, N. Berardi, L. Domenici, L. Maffei, *Vision Res.* **34**, 709 (1994).
22. J. N. Jovanovic et al., *Proc. Natl. Acad. Sci. U.S.A.* **93**, 3679 (1996).
23. J. P. Adams et al., *J. Neurochem.* **75**, 2277 (2000).
24. C. H. Bailey et al., *Neuron* **18**, 913 (1997).
25. T. A. Pham, S. Impey, D. R. Storm, M. P. Stryker, *Neuron* **22**, 63 (1999).
26. A. J. Silva, J. H. Kogan, P. W. Frankland, S. Kida, *Annu. Rev. Neurosci.* **21**, 127 (1998).
27. Supported by Ministero Universita e della Ricerca Scientifica e Tecnologica Cofinanziamento, CNR targeted project in Biotechnology SP-5, Progetto Strategico Neuroscienze, and Progetto Telethon 934.

17 January 2001; accepted 9 May 2001

## Intracellular Anions as the Voltage Sensor of Prestin, the Outer Hair Cell Motor Protein

Dominik Oliver,<sup>1</sup> David Z. Z. He,<sup>2</sup> Nikolaj Klöcker,<sup>1</sup> Jost Ludwig,<sup>1</sup> Uwe Schulte,<sup>1</sup> Siegfried Waldegger,<sup>3</sup> J. P. Ruppersberg,<sup>1</sup> Peter Dallos,<sup>4</sup> Bernd Fakler<sup>1\*</sup>

Outer hair cells (OHCs) of the mammalian cochlea actively change their cell length in response to changes in membrane potential. This electromotility, thought to be the basis of cochlear amplification, is mediated by a voltage-sensitive motor molecule recently identified as the membrane protein prestin. Here, we show that voltage sensitivity is conferred to prestin by the intracellular anions chloride and bicarbonate. Removal of these anions abolished fast voltage-dependent motility, as well as the characteristic nonlinear charge movement ("gating currents") driving the underlying structural rearrangements of the protein. The results support a model in which anions act as extrinsic voltage sensors, which bind to the prestin molecule and thus trigger the conformational changes required for motility of OHCs.

Electromotility of OHCs (1, 2) occurs at acoustic frequencies and is assumed to produce the amplification of vibrations in the cochlea that enables the high sensitivity and frequency selectivity of the mammalian hearing organ (3, 4). This motility results from a protein in the OHC basolateral membrane that undergoes a structural rearrangement in response to changes in the transmembrane voltage (5–7). Coupling of motility and transmembrane voltage is mediated by a charged

voltage sensor within the protein that moves through the electrical field and thus gives rise to a gating current similar to that observed in voltage-gated ion channels (8, 9). Recently, the gene coding for an integral membrane protein of OHCs termed prestin (Fig. 1A) has been identified (10). Upon heterologous expression, the protein reproduces all hallmarks of the motor protein including voltage-dependent charge movement and cell motility (10–13). Because of its fundamental role in OHC electromotility, we examined the mechanism underlying the voltage sensitivity of prestin.

Functionality of the voltage sensor of prestin was probed by measuring the nonlinear capacitance ( $C_{nonlin}$ ) arising from its gating currents with the phase-tracking technique (14). Prestin-expressing CHO cells exhibited a bell-shaped  $C_{nonlin}$  in response to the transmembrane voltage ramped from

–130 mV to 60 mV (Fig. 1B). This electrical signature was well fitted with the derivative of a first-order Boltzmann function [Eq. 1 in (14)] yielding values for  $V_{1/2}$  and  $\alpha$  of  $-75.5 \pm 9.1$  mV and  $35.5 \pm 2.3$  mV ( $n = 16$ ), respectively.

In contrast, no  $C_{nonlin}$  was observed in cells expressing SLC26A6 (15) ( $n = 12$ ), another member of the family of pendrin-related transporters that exhibits closest homology to prestin (~40% identity). It is thus likely that the voltage sensor of prestin is made up of a charged residue present in the prestin sequence but absent in SLC26A6. We mutated each of the nonconserved negatively or positively charged residues in the putative membrane domain of the prestin molecule to a neutral amino acid, glutamine or asparagine, either individually or in groups [(16) and Fig. 1A]. In no case was the electrical signature of the voltage sensor abolished, although in some prestin mutants  $C_{nonlin}$  was shifted along the voltage axis by up to 100 mV (Fig. 1, B and C). The slope factor  $\alpha$  characterizing the voltage dependence of  $C_{nonlin}$  was not significantly different between wild type and any of the mutants tested (17).

These mutagenesis results led to the idea that, instead of being an intrinsic property of the prestin molecule, the voltage sensor may be a charged particle extrinsic to the protein. We thus replaced cations and anions on either side of the membrane by *N*-methyl-D-glucamine (NMDG<sup>+</sup>) or tetra-ethyl-ammonium (TEA<sup>+</sup>) and pentane-sulfonate or sulfate, respectively.  $C_{nonlin}$  of a prestin-expressing CHO cell largely decreased on reduction of the Cl<sup>–</sup> concentration in the whole-cell recording pipette from 150 mM to 2 mM (Fig. 2, A and B). This decrease was fully reversible, as  $C_{nonlin}$  was completely restored when Cl<sup>–</sup> was increased back to 150 mM (Fig. 2B).

<sup>1</sup>Department of Physiology II, University of Tübingen, 72074 Tübingen, Germany. <sup>2</sup>Boys Town National Research Hospital, Omaha, NE 68131, USA. <sup>3</sup>Centre of Pediatrics, University of Marburg, 35037 Marburg, Germany. <sup>4</sup>Auditory Physiology Laboratory, Department of Neurobiology and Physiology, Northwestern University, Evanston, IL 60208, USA.

\*To whom correspondence should be addressed. E-mail: bernd.fakler@uni-tuebingen.de